

An FFT based Bias Voltage Control Scheme to Compensate for the Resonant Frequency Drift of CMUTs Due to Fluid Loading

Thasnim Mohammed, Sazzadur Chowdhury
 Department of Electrical and Computer Engineering
 University of Windsor
 Windsor, Ontario, Canada
 mohamm43@uwindsor.ca, sazzadur@uwindsor.ca

Abstract—This paper presents a Fast Fourier transform (FFT) based bias voltage control scheme to compensate for the resonant frequency drift of Capacitive Micromachined Ultrasonic Transducers (CMUTs) due to fluid loading. A unified mathematical model for the resonant frequency of a CMUT that includes the electrostatic spring softening effect and the fluid loading effect due to the coupled fluidic layer has been developed that provides the basis of the proposed approach. The actual resonant frequency drift has been obtained by comparing the center frequencies of transmitted and received signals extracted through analog-to-digital conversion (ADC) and subsequent FFT of both signals. The frequency drift is then compensated by dynamically adjusting the DC bias voltage that modifies the electrostatic spring softening parameter. Analytical and COMSOL based 3D Finite Element Analysis (FEA) results show that the drift in the resonant frequency of a 6 MHz CMUT operated in water can be compensated by adjusting the bias voltage by 2% from its 75% pull-in voltage value to render an improvement of 4% in lateral and axial resolutions in imaging applications. A bias voltage adjustment of 9% of the 75% pull-in voltage value is necessary to achieve an improvement of 20.74% when the CMUT is operated in glycerol. The scheme can be realized using standard commercially available microelectronic components to improve the accuracy and reliability of diagnostic imaging and non-destructive evaluation (NDE).

Keywords—CMUT; electrostatic spring softening; fluid loading effect; resonant frequency drift; FFT-based microelectronic compensation.

I. INTRODUCTION

Fluid loading induced resonant frequency drift of capacitive micromachined ultrasonic transducers (CMUTs) challenge their applications in biomedical imaging, non-destructive evaluation (NDE), and high intensity focused ultrasound (HIFU) applications [1]–[4]. Specifically, the phenomenon contributes to lower imaging resolution and beamforming functionality compared to the piezoelectric ultrasonic transducers. A suitable solution to the problem is necessary to exploit the significant advantages of CMUTs over the piezoelectric ones, such as low cost fabrication, easier CMOS integration, improved signal-to-noise ratio, higher fractional bandwidth, and thermal stability.

The CMUT is basically a reciprocal electrostatic transducer that relies on capacitance change between a

movable and a fixed electrode separated by a small gap to generate or receive ultrasound [5][6]. The space between the electrodes is filled with either vacuum or a thin film of air. The movable electrode (typically a thin diaphragm) is supported at the edges by dielectric support posts.

When a CMUT array operates in a fluidic medium, the coupled fluidic layer manifests itself as an inertial mass onto the diaphragm and as a viscous damper depending on the viscosity of the fluidic medium. As these fluid loading effects alter the effective mass of the CMUT diaphragm, a drift of the resonant frequency of the CMUT occurs. Since the elements in a CMUT array are designed to have a fixed pitch to satisfy the Nyquist criteria of spatial sampling in beamforming operations, a change in the CMUT resonant frequency compromises the functional characteristics of the array.

Attempts to mitigate the fluid loading effects and thereby minimize the center frequency drift of CMUT arrays are diverse in nature but not too many [7]–[17]. Notably, the effects of fluid loading and waveguiding on the performance of a CMUT array were addressed in an analytical model presented in [7], where frequency dependent equivalent density was used as the effective CMUT diaphragm material density to account for the distributed fluid loading. The authors in [7] also presented the dimensional dependence of the equivalent density using a finite element method (FEM) model based data fitting technique. In [8], the acoustic parameters for an array consisting of parallel driven CMUT cells were derived as a complex mechanical fluid impedance that depends on the diaphragm shape function. As the CMUTs in [8] were modeled as piston radiators, the model lacks sufficient accuracy. The authors in [9] presented a generalized model for surface acoustic wave devices considering the mass and viscous fluid loading. The authors presented the frequency and phase changes occurring when the device is operated in immersion and the dependence of the frequency drift on the fluid properties was included to analyze the fluid loading effect. Numerical modeling of fluid interaction with oscillating surfaces is available in [10] from which reduced order models depicting the fluid interaction were developed based on the effective fluid volume, effective area of shear wave interaction, and effective length of viscous interaction. The sensitivity of CMUT equivalent circuit parameters to the fluid properties was investigated in [11], where a surface acoustic wave (SAW) device was

designed for sensing the fluid properties like mass density and viscosity. The phenomenon of drift in frequency of CMUTs operated in immersion or in contact with a fluid medium has been exploited to develop various biological and chemical sensing devices [12]–[17].

In this perspective, this paper presents a method to compensate the resonant frequency drift of a CMUT due to fluid loading by dynamically adjusting the DC bias voltage. The scientific basis of the proposed method lies in the spring softening effect associated with the DC bias voltage applied to a CMUT. Due to an applied DC bias, necessary for CMUT operation in both transmit and receive modes, the effective stiffness of the diaphragm reduces to lower the resonant frequency. As the amount of spring softening (lowering of the stiffness) depends on the DC bias, the DC bias voltage can be dynamically controlled using a suitable microelectronic circuit to adjust the spring softening amount to offset the effect of fluid loading on the resonant frequency. Excellent agreements between lumped element model analysis and 3D electromechanical finite element analysis conducted by the authors show that the method can effectively offset the resonant frequency drift due to fluid loading to validate the hypothesis. A microelectronics based compensation scheme to implement the proposed hypothesis has been designed and simulated using MATLAB and Simulink. The simulation results validate the efficacy of the proposed method, thereby proving the hypothesis.

The rest of the paper has been organized in the following manner: Section II provides the problem statement and theoretical background of the proposed approach, Section III investigates the effect of fluid loading on CMUT resonant frequency in different fluids, Section IV presents the proposed frequency drift compensation method with simulation results of analytical and FEA analysis using COMSOL, Section V presents the design of microelectronics based compensation scheme along with simulation results and finally, Section VI provides the concluding remarks.

II. THEORETICAL BACKGROUND

A CMUT array is comprised of several transmit and receive elements as shown in Figure 1(a). Each element in turn is designed to have several CMUT cells connected in parallel [10][18]–[21]. A conceptual cross-section of a typical CMUT cell is shown in Figure 1(b).

Assuming the CMUT as a lumped element mass-spring-dashpot system with a linear spring constant, the resonant frequency of the CMUT in air can be calculated following

$$f_{\text{res}} = \frac{1}{2\pi} \sqrt{\frac{k}{m}} \quad (1)$$

where, k and m are the spring constant (stiffness) and mass of the CMUT diaphragm as shown in Figure 1(b), respectively.

The array pitch, defined as the distance between corresponding points in the neighboring elements (Figure 1(a)), is optimized to satisfy Nyquist criteria of spatial sampling as expressed in (2) to minimize grating lobes.

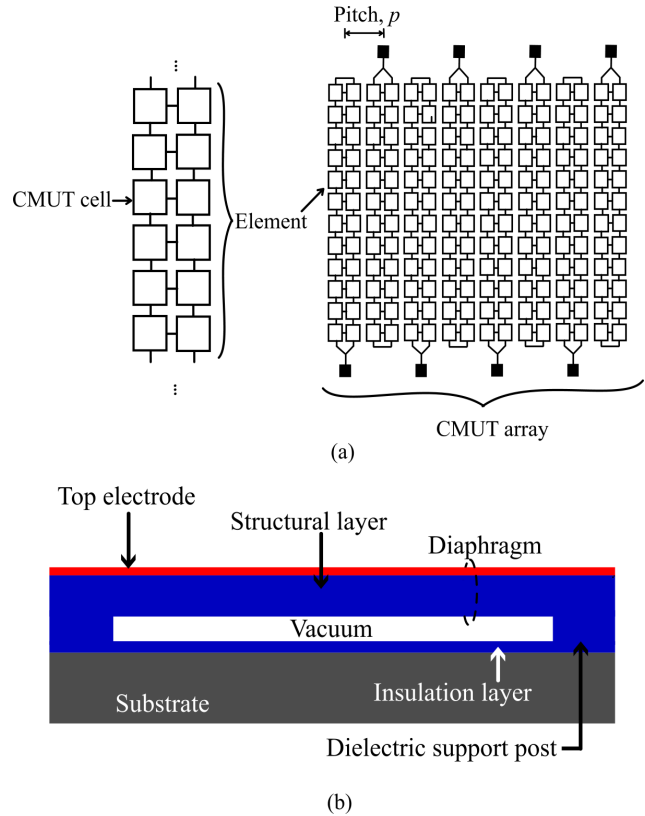


Figure 1. (a) Layout of a CMUT array comprising of array elements. (b) Typical cross-section of a single CMUT cell.

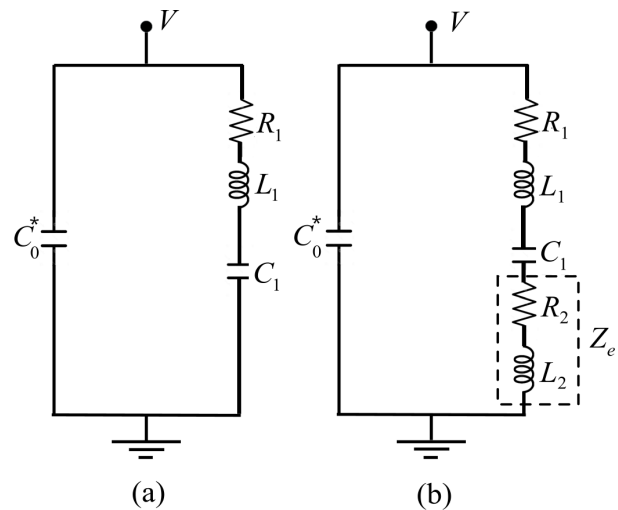


Figure 2. (a) The BVD model of a CMUT without fluid loading. (b) The BVD model of a CMUT with fluid loading. The fluid loading effect is represented by inductance L_2 and resistance R_2 .

$$p \leq \frac{\lambda}{2} \quad (2)$$

In (2), λ is the wavelength corresponding to the center frequency of operation.

The frequency response of a CMUT cell with and without the fluid loading effect can be obtained using the Butterworth-Van Dyke (BVD) model as shown in Figure 2. [22]. The BVD model depicts an analog electrical equivalent circuit of a CMUT that includes both electrical and equivalent mechanical lumped element circuit parameters.

In the BVD model of a CMUT, the electrical circuit element is represented by a lumped capacitor C_0^* , and the electrical equivalent of mass m , stiffness k , and damping element b is represented by L_1 , C_1 , and R_1 respectively.

Typically, the CMUT diaphragms are constructed to have a circular, hexagonal, or square shape geometry to satisfy the design requirements. For a CMUT with a square diaphragm in the small deflection regime, the stiffness k of the diaphragm can be calculated following

$$k = C_r \frac{t_d \sigma_0}{(L/2)^2} + C_b \frac{12D_{\text{eff}}}{(L/2)^4} \quad (3)$$

where $C_r = 3.45$ and $C_b = 4.06$ [23]. The parameters D_{eff} , L , σ_0 , and t_d are the effective flexural rigidity, sidelength, residual stress, and thickness of the diaphragm, respectively. The mass of the diaphragm can be calculated from the volume and density of the CMUT diaphragm materials. The parameters R_1 , L_1 , and C_1 (zero bias equivalent stiffness) can be calculated from [22],

$$\begin{cases} C_1 = \frac{n^2}{k} \\ L_1 = \frac{m}{n^2} \\ R_1 = \frac{b}{n^2} \end{cases} \quad (4)$$

where, n is the electromechanical transformation ratio given by:

$$n = \frac{\epsilon_0 A V_{\text{DC}}}{(d_{\text{eff}} - x)^2} \quad (5)$$

In (5), ϵ_0 , A , V_{DC} , x and d_{eff} denote the free-space permittivity, coupling area of the electrodes, DC bias voltage applied to the CMUT, average diaphragm deflection, and the effective electrode gap, respectively.

During immersion operation in a liquid medium, the coupled liquid layer contributes an additional equivalent damping R_2 due to the fluid viscosity and an additional equivalent fluid mass L_2 . This phenomenon alters the

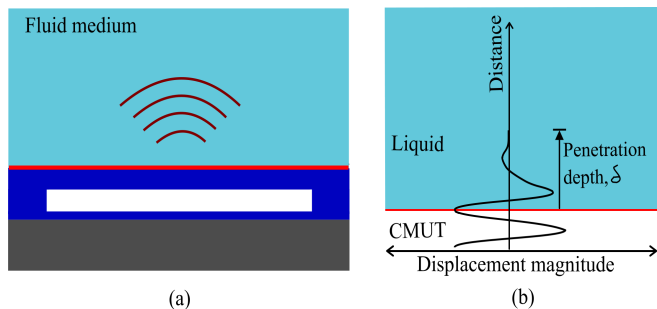


Figure 3. (a) Cross sectional view of CMUT contacted by liquid on one side (b) The penetration depth of shear wave propagated into the liquid medium.

CMUT motional impedance contributed originally by L_1 , C_1 , and R_1 .

The inclusion of these additional mass and damping parameters in the BVD model as shown in Figure 2(b) alters the frequency response of the CMUT. The amount of alteration (drift) depends on the density and viscosity of the fluidic medium.

The fluid loading quantities L_2 and R_2 can be calculated by accounting the penetration depth δ of the damped shear wave propagating into the liquid due to the coupled oscillating surface (CMUT diaphragm) as shown in Figure 3. Following [22][24], the penetration depth δ can be calculated from the relation $\delta = \sqrt{2\eta / \omega_s \rho}$ where, ρ , η , and ω_s represents the liquid density, shear viscosity of the liquid, and resonant frequency of the CMUT in rad/sec, respectively. The effective height $\delta/2$ of the entrained liquid layer can thus be used to calculate the fluid loading quantities L_2 and R_2 following [22] as

$$L_2 = \frac{\pi}{4k_s^2 \omega_s C_0} \left(\frac{\rho \eta}{2\omega_s \mu_q \rho_q} \right)^{\frac{1}{2}} \quad (6)$$

$$R_2 = \frac{\pi}{4k_s^2 C_0} \left(\frac{\rho \eta}{2\omega_s \mu_q \rho_q} \right)^{\frac{1}{2}} \quad (7)$$

where μ_q , ρ_q , and k_s^2 represents the diaphragm shear stiffness, mass density of diaphragm, and coupling coefficient, respectively.

Thus, the motional impedance Z_m in the BVD model of a CMUT including the fluid loading effect (Figure 2(b)) can be calculated from:

$$Z_m = R_1 + R_2 + j\omega L_1 + j\omega L_2 + \frac{1}{j\omega C_1} \quad (8)$$

On the other hand, assuming the small-signal model of a CMUT where the AC actuation signal is much smaller compared to the DC bias voltage ($V_{DC} \gg V_{AC}$), the spring softening effect due to an applied DC bias voltage reduces the zero bias CMUT diaphragm stiffness k by a factor k_{soft} as given by

$$k_{soft} = \frac{\epsilon_0 A V_{DC}^2}{d_{eff}^3} \quad (9)$$

Consequently, the spring softening effect causes a downshift of the resonant frequency of the CMUT diaphragm following

$$f_{res-ss} = \frac{1}{2\pi} \sqrt{\frac{k - k_{soft}}{m}} \quad (10)$$

During an immersion operation, the resonant frequency f_{res-ss} as expressed in (10) is further affected by the inertial mass m_f contributed by the coupled fluid layer adjacent to the CMUT diaphragm.

Thus, including both the spring softening effect and the fluid loading effect, the resonant frequency $f_{res-ss-fl}$ of the diaphragm can be expressed as

$$f_{res-ss-fl} = \frac{1}{2\pi} \sqrt{\frac{k - k_{soft}}{m + m_f}} \quad (11)$$

A careful examination of (9) and (11) reveals that the drift in the resonant frequency due to the fluid loading effect m_f alone can be minimized by adjusting the spring softening factor k_{soft} , which is a function of the bias voltage V_{DC} in small-signal approximation.

A microelectronic circuit can be designed to sense the resonant frequency offset and adjust the bias voltage dynamically to control k_{soft} to bring the resonant frequency back to its design value while generating the desired acoustic outputs.

III. INVESTIGATION OF FLUID LOADING EFFECTS

To investigate the proposed approach, a linear CMUT array with a center frequency of 6 MHz has been considered. This center frequency is suitable for cardiac diagnostic imaging as reported in [25].

A. Analytical CMUT Resonant Frequency Calculation with Fluid Loading Effects

Individual CMUT cells in the array have been designed to have the same resonant frequency as the array [26]. The element pitch p has been selected following (2) to satisfy the Nyquist criteria of spatial sampling to obtain better

directivity with minimum side lobes. The lateral and axial resolutions of the CMUT array are given by [2] as:

$$\Delta y = \left(\frac{1.22\lambda}{A_a} \right) S \quad (12)$$

$$\Delta x = \frac{n\lambda}{2} \quad (13),$$

respectively, where A_a , S , and n are the array aperture, the distance between the focus and the array surface at the center of the array, and the number of scanning pulses, respectively. Following (12) and (13), it is necessary for the CMUT and the array physical dimensions to correspond to the same wavelength or center frequency to achieve setpoint axial and lateral resolutions and avoid any deviation from Nyquist criteria of spatial sampling [27][28].

To investigate the effects of viscosity and density of the fluidic medium on the resonant frequency of the CMUT diaphragms, a square shaped CMUT diaphragm with the same 6 MHz center frequency in air as for the array has been investigated.

Typical CMUT diaphragms are fabricated as a multilayer laminate where a thin insulating material is used as the structural layer to provide the necessary mechanical strength and a thin conducting layer is used on the top of the structural layer to act as the top electrode.

Following [27], bisbenzocyclobutene (BCB) has been used as the structural layer for this analysis. The BCB layer is coated with a thin layer of gold to form the top electrode. Low resistivity silicon has been used to constitute the bottom electrode (ground). BCB has also been used to fabricate the dielectric support posts. The major physical properties of the selected CMUT materials are listed in Table I.

TABLE I. CMUT MATERIAL PROPERTIES

Material	Young's modulus (GPa)	Poisson's ratio	Density (kg.m ⁻³)	Residual stress (MPa)
BCB	2.9	0.34	1050	28
Gold	70	0.44	19300	106
Silicon	165.9	0.26	2329	55

TABLE II. GEOMETRICAL SPECIFICATION OF THE CMUT CELL.

Parameter	Value	Unit
Sidelength (L)	28	μm
Diaphragm thickness (d_m)	1.5	μm
Top electrode thickness (t_m)	0.1	μm
Cavity height (d_0)	0.75	μm
Insulation layer thickness (d_i)	0.1	μm

A CMUT cell has been designed using the materials listed in Table I to obtain the target 6 MHz resonant frequency in air. The design incorporates the electrostatic spring softening effect due to the bias voltage. Analytical and 3D electromechanical FEA methods were used to optimize the geometric dimensions as listed in Table II.

The drift in resonant frequency due to the spring softening effect as given by (9) and (10) is shown in Figure 4. The pull-in voltage of the CMUT has been determined from 3D electromechanical FEA using COMSOL as 395 volts. The frequency responses of the CMUT biased at 294.75 volts (74.68% of the pull-in voltage) in air, water, engine oil, and glycerol are shown in Figure 5. The physical properties of the fluids are listed in Table III.

The frequency response in air without any DC bias voltage has also been shown in Figure 5. As it can be seen, there is a significant drift in the resonant frequency due to

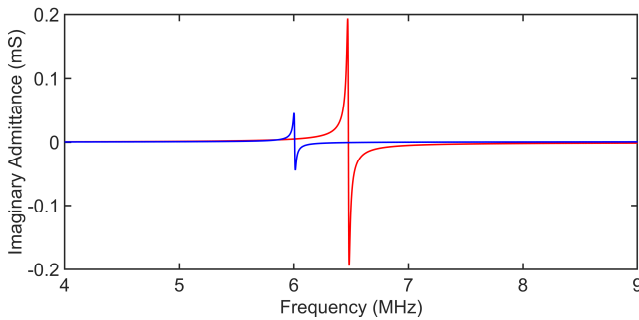


Figure 4. Drift in resonant frequency due to the spring softening effect.

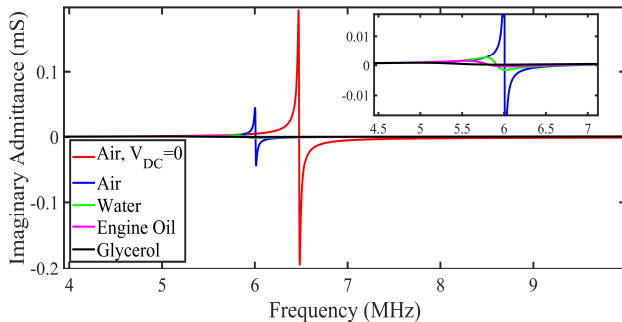


Figure 5. Frequency response of the CMUT cell with bias voltage $V_{DC} = 0.75V_{PI}$ for unloaded (air) and loaded (water, engine oil, glycerol) conditions. (Inset y-axis unit is in μS .)

TABLE III. RESONANT FREQUENCY OF THE SIMULATED CMUT IN DIFFERENT FLUIDS

Medium	Resonant frequency (Analytical) (MHz)	Resonant frequency (FEA) (MHz)	Percentage deviation between analytical and FEA (%)	Drift from the resonant frequency in air (FEA)(%)
Air	6.002	6.19	3.1	-
Water	5.783	5.945	2.8	3.9
Engine oil	5.422	5.545	2.3	10.42
Glycerol	4.975	4.8788	1.9	21.18

the spring softening effect caused by the bias voltage, which is further deteriorated by the fluid loading effects contributed by the fluid mass and viscosity as shown in the zoomed-up inset.

B. 3D FEA Based CMUT Resonant Frequency Simulation with Fluid Loading Effects

A 3D FEA of a single CMUT cell was conducted in COMSOL Multiphysics environment to investigate the fluid loading effects on the frequency response of the CMUT cell. The cell was modeled using the electro-mechanical module as shown in Figure 6. The air/fluid column was designed using the pressure acoustics frequency domain physics module.

The CMUT diaphragm was set as a linear elastic material. The boundary between the electro-mechanics and pressure acoustics domain was defined as a fluid-solid coupled boundary that acts as a pressure load on the electro-mechanics domain. The maximum element size was set to one-sixth of the smallest wavelength in a frequency sweep while meshing. An AC perturbation signal superimposed with DC bias voltage was applied to the CMUT cell using the default frequency domain modal analysis method in COMSOL.

The COMSOL based 3D FEA generated modal frequency responses of the CMUT model for the fluids listed in Table III are shown in Figure 7. Table IV compares the analytical and 3D FEA results for the resonant frequencies of the CMUT in the investigated fluids. As Table IV reveals, the analytical and 3D FEA results are in excellent agreement with a maximum deviation of 2.8% for the liquids that validate the efficacy of the analytical and simulation methods.

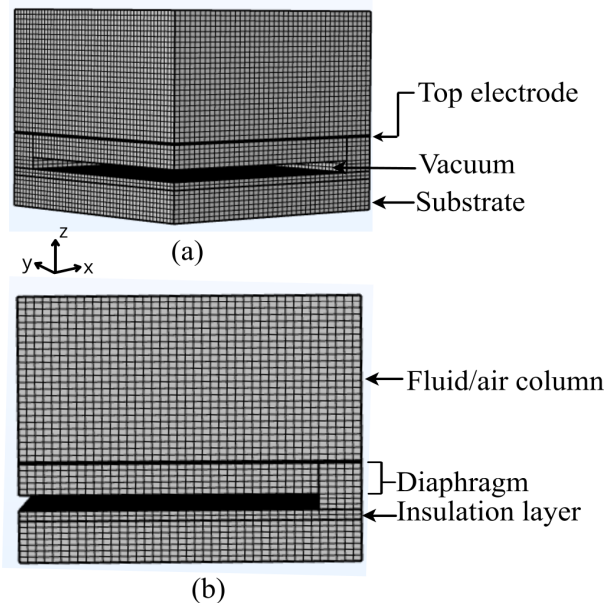


Figure 6. The CMUT model in COMSOL Multiphysics environment (As the structure is symmetric, only a quarter model of the CMUT was simulated).

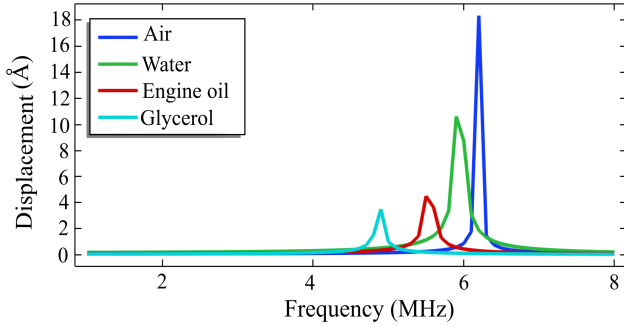


Figure 7. FEA simulation based frequency response of the CMUT cell in different fluids.

TABLE IV. CMUT RESONANT FREQUENCIES IN INVESTIGATED FLUIDS

Fluid type	Fluid Physical Properties		Resonant frequency (MHz)
	Viscosity (mPa/s)	Density (g/cm ³)	
Air	0.01825	0.001204	6.002
Water	1.0016	0.998	5.783
Engine oil	287.23	0.8787	5.422
Glycerol	1412.8	1.2608	4.975

IV. COMPENSATING THE FLUID LOADING EFFECTS

Investigation by the authors reveals that the resonant frequency drift due to the fluid loading effect can be compensated effectively if it is possible to offset the effects of fluid loading by dynamically adjusting the DC bias voltage following (9) and (11). Precisely, the spring softening parameter k_{soft} as expressed in (9) needs to be dynamically adjusted by adjusting the bias voltage V_{DC} , to offset the fluid loading induced resonant frequency drift Δf expressed in (14).

$$\Delta f = f_{\text{res-ss}} - f_{\text{res-ss-fl}} \quad (14)$$

Figures 8-10 compare uncompensated (red) and DC bias compensated (black) frequency responses of the CMUT when operated in different fluidic media. From the figures, it is clear that a slight adjustment of the DC bias, (e.g., $0.75 V_{\text{PI}}$ to $0.68 V_{\text{PI}}$ for glycerol) is sufficient to alter the electrostatic spring softening parameter to offset the resonant frequency drift due to the mass loading.

COMSOL based 3D FEA simulation results after adjusting the bias voltage to offset the resonant frequency drift Δf for water, engine oil, and glycerol are shown in Figures 11-13. The reference bias voltage was kept at 75%, of the pull-in voltage V_{PI} of the CMUT structure as in the Section III. When the CMUT was operated in water, engine

oil, and glycerol, the change in bias voltage applied was 2%, 4.2%, and 9%, respectively. The simulation results confirm that the drift Δf in the resonant frequency can effectively be compensated by a small change in the DC bias V_{DC} to validate the hypothesis.

The improvement in the lateral and axial resolution that could be achieved with the proposed method is 4%, 10.78%, 20.74% when operated in water, engine oil, or glycerol, respectively. Thus, the proposed method helps to achieve the expected resolution even when the array is operated in different fluidic mediums, thereby improving the imaging accuracy of a CMUT array.

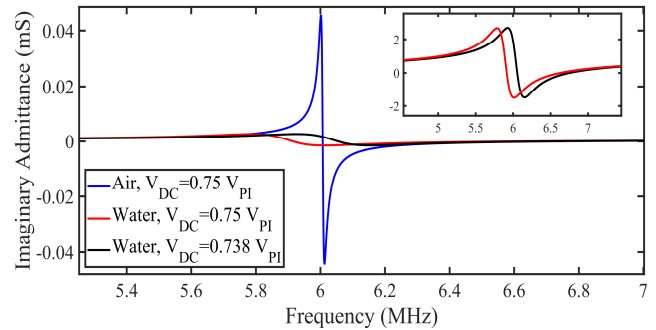


Figure 8. Simulation result of CMUT small-signal analysis for frequency compensation in water. (Inset y-axis unit is in μS .)

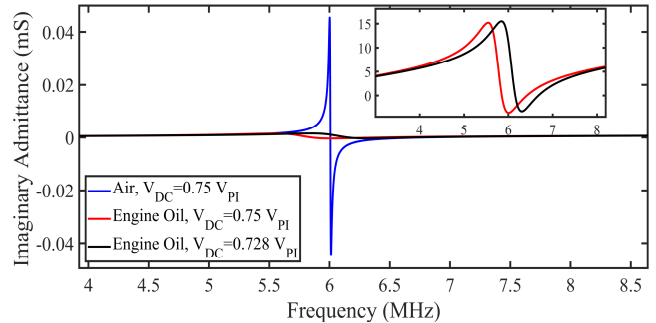


Figure 9. Simulation result of CMUT small-signal analysis for frequency compensation in engine oil. (Inset y-axis unit is in μS .)

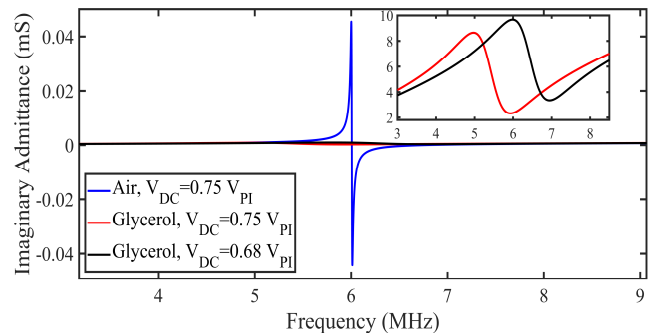


Figure 10. Simulation result of CMUT small-signal analysis for frequency compensation in glycerol. (Inset y-axis unit is in μS .)

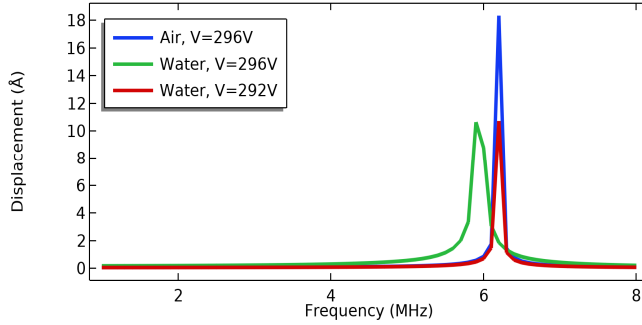


Figure 11. FEA simulation result for frequency compensation in water

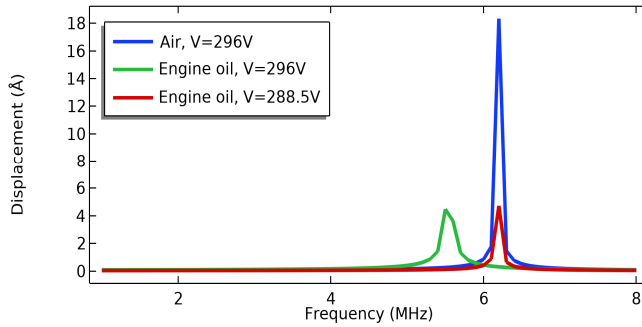


Figure 12. FEA simulation result for frequency compensation in engine oil.

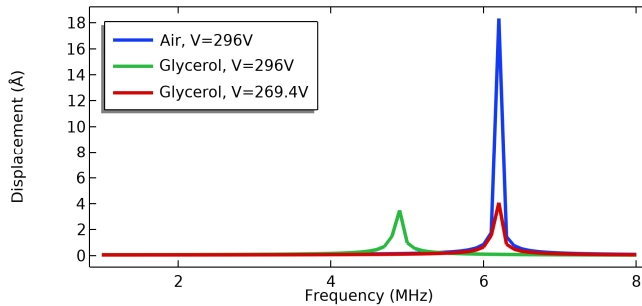


Figure 13. FEA simulation result for frequency compensation in glycerol.

V. COMPENSATION SCHEME IMPLEMENTATION

An implementation method as shown in Figure 14 to realize the proposed compensation scheme has been developed and simulated using a Simulink based model. The model incorporates commercially available analog-to-digital converters (ADC), fast Fourier transform (FFT) modules, and bandpass filters among others, to dynamically determine the drift amount and apply necessary compensation to stabilize the center frequency using a digital signal processing (DSP) based algorithm.

A. Implementation Strategy

The actual drift amount in the resonant frequency of a CMUT during an array operation can be determined by comparing the center frequencies of the transmitted and the

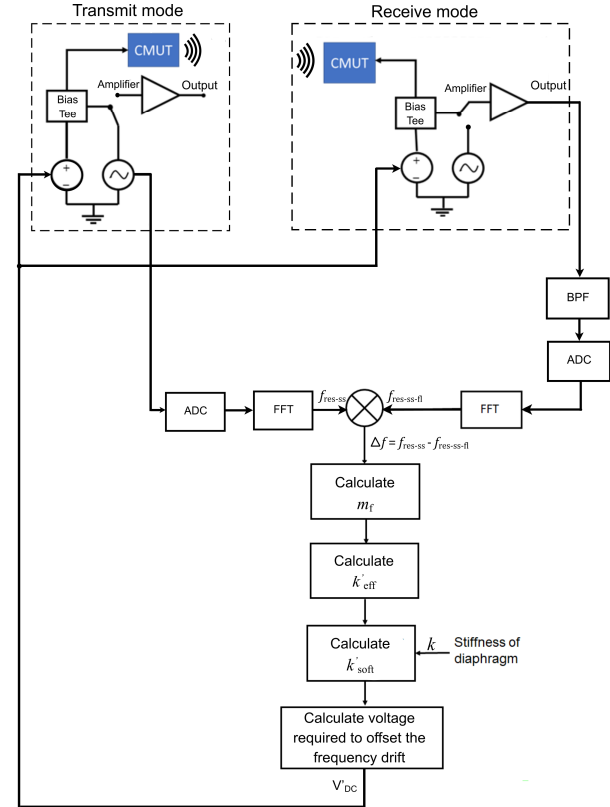


Figure 14. Block diagram of the compensation scheme.

received signals. While the center frequency of the transmitted signal can easily be extracted from the excitation AC signal applied to the CMUT, appropriate conditioning of the received signal is necessary to extract the center frequency component of the received signal. Accordingly, a bandpass filter is necessary to signal-condition the received signal before converting to frequency domain. To extract the center frequencies, the AC excitation signal and the filtered received signal are digitized using high-speed analog-to-digital converters (ADC) with a suitable sampling rate.

The time-domain digitized signals are then transformed into frequency domain using fast Fourier transforms (FFT) to obtain center frequencies in both signals (f_{res-ss} and $f_{res-ss-fl}$ in Figure 14). A comparator then compares f_{res-ss} and $f_{res-ss-fl}$ to determine the frequency drift Δf in real time.

The mass m_f of the loaded fluidic layer is then extracted from Δf using (10) and (11) as the other parameters in (10) and (11) are already known. The compensation scheme then calculates a modified effective stiffness k'_{eff} to offset the effects of m_f in (11). A new value of the spring softening parameter k'_{soft} is then extracted from k'_{eff} following

$$k'_{eff} = k - k'_{soft}. \quad (15)$$

Finally, the modified value of DC bias voltage V'_{DC} is extracted from k'_{soft} following (9) as

$$V'_{DC} = \sqrt{\frac{k'_{soft} d_{eff}^3}{\epsilon_0 A}} \quad (16)$$

The compensation module applies the modified bias voltage V'_{DC} to the CMUT through the bias tee as shown in Figure 14.

B. Scheme Validation

The proposed scheme as shown in Figure 14 was implemented and simulated in MATLAB and Simulink. First, a bandpass filter was used to remove the noise from the received signal. Next, both the AC excitation signal and the filtered received signal are sampled at a frequency, $f_{sampling} \geq 2f_{res-ss}$ (15 MHz for the designed 6 MHz array) to digitize them. The digitized signals are then fast Fourier transformed to extract the frequency components. The spectra of the digitized signals after performing FFT for operation in water are compared in Figure 15. Similarly, the spectra of the digitized signals after performing FFT for operation in engine oil and glycerol are compared in Figures 16-17, respectively. The drift in center frequency due to fluid loading is clearly visible in the figures with higher density and viscosity medium (glycerol) showing higher drift compared to lower density and viscosity medium (water).

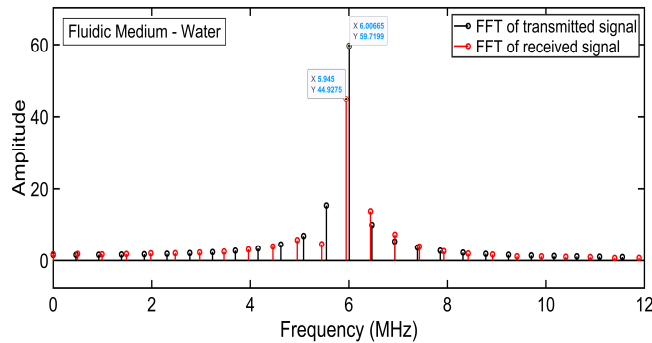


Figure 15. FFT of the filtered received signal when operated in water.

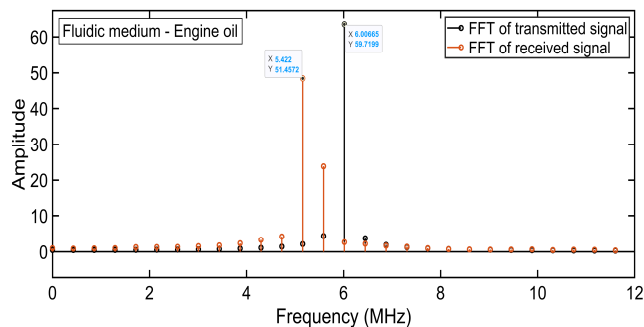


Figure 16. FFT of the filtered received signal when operated in engine oil.

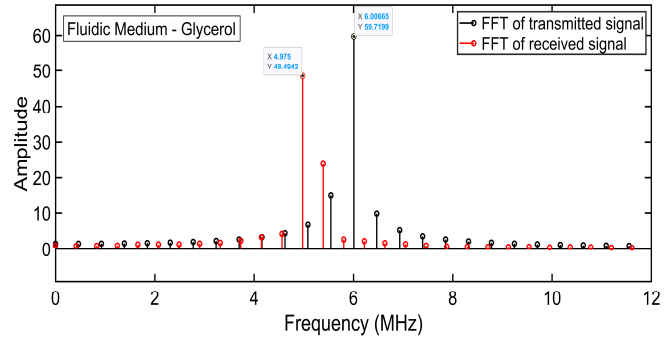


Figure 17. FFT of the filtered received signal when operated in glycerol.

Based on the magnitude of drift in center frequency, a modified DC bias voltage V'_{DC} is then calculated for each case following (14) – (16) to adjust the spring softening parameter to offset the fluid loading effect. The spectra of the filtered and digitized received signals with V'_{DC} after FFT are shown in Figure 18. for all three cases along with the spectra of the transmit AC signal. As it can be seen, the adjustment of the DC bias compensates the frequency drift as expected.

The amount of V'_{DC} in different fluidic media is different corresponding to the different amount of drift in different fluidic media. TABLE V. compares MATLAB and Simulink predicted V'_{DC} following the proposed scheme with the uncompensated DC bias V_{DC} for different fluidic media. Similarly, V'_{DC} obtained from 3D FEA simulation in COMSOL are compared in Table VI with uncompensated DC bias for different fluidic media.

The tables show that the variations in DC bias are very small to minimally affect the target acoustic pressure. Furthermore, Tables V and VI show that the analytical results obtained from the simulated scheme in Matlab and Simulink are in excellent agreement with 3D FEA results to validate the implementation scheme.

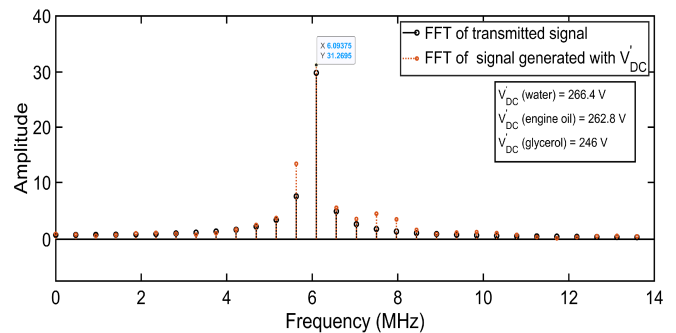


Figure 18. Comparison of FFT of the transmit and received signals after DC bias adjustment from V_{DC} to V'_{DC} .

TABLE V. COMPARISON OF DC BIAS ADJUSTMENT REQUIRED TO OFFSET THE FREQUENCY DRIFT IN MATLAB/SIMULINK

Medium	DC bias voltage (V_{DC}) (V)	Modified DC voltage (V'_{DC}) (V)	Percentage deviation (%) $\frac{V_{DC} - V'_{DC}}{V_{DC}}$
Water	270.675	266.43	1.56
Engine oil	270.675	262.8125	2.9
Glycerol	270.675	246	9.11

TABLE VI. COMPARISON OF DC BIAS ADJUSTMENT REQUIRED TO OFFSET THE FREQUENCY DRIFT IN COMSOL

Medium	DC bias voltage (V_{DC}) (V)	Modified DC voltage (V'_{DC}) (V)	Percentage deviation (%) $\frac{V_{DC} - V'_{DC}}{V_{DC}}$
Water	294.75	292	0.93
Engine oil	294.75	288.5	2.12
Glycerol	294.75	269.4	8.6

VI. CONCLUSION

Microelectronic and digital signal processing techniques have been used to compensate fluid loading induced resonant frequency drift of a CMUT by dynamically adjusting the DC bias voltage. Analytical and 3D FEA based simulation studies revealed that the magnitude of DC bias voltage adjustment is small and is not expected to affect the acoustic power/pressure output of a CMUT array while improving lateral and axial resolution. The investigation shows that the method can improve the lateral and axial resolutions in water by approximately 4% to improve the accuracy of CMUT based biomedical diagnostic imaging. For NDE applications, the axial and lateral resolution improvements can be as high as 20.74% when glycerol is used as the coupling agent.

MATLAB and Simulink based simulation of the proposed scheme shows that commercially available high-speed data converters and digital signal processing (DSP) integrated circuits can be used to determine the frequency drift using Fast Fourier Transform (FFT) of the digitized transmit and the processed received signal. A DSP based controller can then dynamically compute and apply the modified DC bias to offset the frequency drift. High-speed signal processing components are necessary to minimize the latency time. The compensation scheme will be realized and tested once necessary funding is available.

ACKNOWLEDGMENT

This research work was supported by the Natural Science and Engineering Research Council of Canada (NSERC)'s discovery grant number RGPIN 293218. The authors also

acknowledge the collaborative research support provided by the IntelliSense Corporation, Lynnfield, MA, Angstrom Engineering, ON, and the CMC Microsystems, Canada.

REFERENCES

- [1] T. Mohammed and S. Chowdhury, "A Method to Minimize Resonant Frequency Drift of CMUTs Due to Fluid Loading", *SENSORDEVICES 2021, The Twelfth International Conference on Sensor Device Technologies and Applications*, ISSN: 2308-3514, pp. 88-91, November 2021. Available online: https://www.thinkmind.org/index.php?view=article&articleid=sensor_devices_2021_2_120_20053
- [2] J. Song et al. "Capacitive Micromachined Ultrasonic Transducers (CMUTs) for Underwater Imaging Applications," *Sensors*, vol. 15, no. 9, pp. 23205–23217, Sep. 2015.
- [3] D. Zhao, S. Zhuang, and R. Daigle, "A commercialized high frequency CMUT probe for medical ultrasound imaging," in *Proc. of 2015 IEEE International Ultrasonics Symposium (IUS)*, Oct. 21-24, Taipei, Taiwan, 2015, pp. 1-4.
- [4] A. S. Ergun, G. G. Yarlioglu, O. Oralkan, and B. T. Khuri-Yakub, "Chapter 7: Techniques & Applications of Capacitive Micromachined Ultrasonic Transducer," in *MEMS/ NEMS Handbook[Techniques and Applications]*; Leondes, C.T., Ed.; Springer Science + Business Media Inc.: Los Angeles, CA, USA, 2006; Volume 2, pp. 222–332.
- [5] A. S. Ergun, G. G. Yarlioglu, and B. T. Khuri-Yakub, "Capacitive micromachined ultrasonic transducers: Theory and technology." *Journal of aerospace engineering*, vol 16, no. 2, pp. 76-84, 2003.
- [6] Y. Huang, A. S. Ergun, E. Haeggstrom, M. H. Badi, and B. T. Khuri-Yakub, "Fabricating capacitive micromachined ultrasonic transducers with wafer-bonding technology," *Journal of Microelectromechanical Systems*, vol. 12, no. 2, pp. 128-137, April 2003.
- [7] B. Azmy, M. El-Gamal, A. El-Henawy, and H. Ragai, "An accurate model for fluid loading on circular CMUTs," in *Proc. of 2011 IEEE International Ultrasonics Symposium*, Orlando, Florida, Oct. 18-24, 2011, pp. 584-587.
- [8] A. Lohfink, P. -. Eccardt, W. Benecke, and H. Meixner, "Derivation of a 1D CMUT model from FEM results for linear and nonlinear equivalent circuit simulation," in *Proc. of 2003 IEEE Ultrasonics Symposium*, Honolulu, Hawaii, Oct. 5-8, 2003 pp. 465-468.
- [9] M. Tsai and J. Jeng, "Development of a generalized model for analyzing phase characteristics of SAW devices under mass and fluid loading," in *IEEE Transactions on Ultrasonics, Ferroelectrics, and Frequency Control*, vol. 57, no. 11, pp. 2550-2563, November 2010.
- [10] E. K. Reichel, M. Heinisch, B. Jakoby, and T. Voglhuber-Brunnmaier, "Efficient numerical modeling of oscillatory fluid-structure interaction," in *Proc. of IEEE SENSORS 2014*, Valencia, Spain, Nov. 2-5, 2014, pp. 958-961,
- [11] M. Thränhardt, P. Eccardt, H. Mooshofer, P. Hauptmann, and L. Degertekin, "A resonant CMUT sensor for fluid applications," in *Proc. of IEEE SENSORS 2009, Christchurch, New Zealand, 25-28 October, 2009*, pp. 878-883.
- [12] S. Eaimkhong, M. Steiert, T. Harper, M. Cable, and J. Gimzewski, "Label-Free Biodetection Using Capacitive Micromachined Ultrasonic Transducers (CMUTs) and Its Application for Cardiovascular Disease Diagnostics". *J Nanomed Nanotechol.* 3. No. 144, 2012.
- [13] B. T. Khuri-Yakub et al., "6D-1 The Capacitive Micromachined Ultrasonic Transducer (CMUT) as a Chem/Bio Sensor," 2007 IEEE Ultrasonics Symposium Proceedings, New York, NY, 2007, pp. 472-475, doi: 10.1109/ULTSYM.2007.127.
- [14] Z. Li, L. Zhao, Z. Jiang, Z. Ye and Y. Zhao, "Capacitive micromachined ultrasonic transducer for ultra-low pressure detection," The 9th IEEE International Conference on Nano/Micro

- Engineered and Molecular Systems (NEMS), Waikiki Beach, HI, 2014, pp. 600-603, doi: 10.1109/NEMS.2014.6908883.
- [15] K. K. Park, H. J. Lee, G. G. Yaralioglu, A. S. Ergun, Ö. Oralkan, M. Kupnik, and J. K. Gimzewski, "Capacitive micromachined ultrasonic transducers for chemical detection in nitrogen". *Applied Physics Letters*, 2007, 91(9), 094102.
- [16] L. Zhao et al., "A Novel CMUT-Based Resonant Biochemical Sensor Using Electrospinning Technology," in *IEEE Transactions on Industrial Electronics*, vol. 66, no. 9, pp. 7356-7365, Sept. 2019, doi: 10.1109/TIE.2018.2878123.
- [17] H. J. Lee, K. K. Park, O. Oralkan, M. Kupnik and B. T. Khuri-Yakub, "CMUT as a chemical sensor for DMMP detection," 2008 IEEE International Frequency Control Symposium, Honolulu, HI, 2008, pp. 434-439, doi: 10.1109/FREQ.2008.4623034.
- [18] H. Wang, X. Wang, C. He, and C. Xue, Design and performance analysis of capacitive micromachined ultrasonic transducer linear array. *Micromachines*, vol. 5, no. 3, pp.420-431, 2014.
- [19] T. Zure, "Characterization of a CMUT Array," Master's Thesis, Dept. of Electrical and Computer Engineering, Univ. of Windsor, Windsor, ON, Canada, 2012.
- [20] V. Yashvanth, "CMUT Crosstalk Reduction Using Crosslinked Silica Aerogel," Master's Thesis, Dept. of Electrical and Computer Engineering, Univ. of Windsor, Windsor, ON Canada, 2018.
- [21] R. Zhang et al., "Design and performance analysis of capacitive micromachined ultrasonic transducer (CMUT) array for underwater imaging." *Microsystem Technologies*, vol. 22, no. 12, pp. 2939-2947, 2016.
- [22] D. S. Ballantine Jr et al., *Acoustic wave sensors: theory, design and physico-chemical applications*. San Diego, CA, USA: Elsevier; 1996.
- [23] M. Rahman and S. Chowdhury, "A new deflection shape function for square membrane CMUT design," in *Proc. of 2010 IEEE International Symposium on Circuits and Systems*, Paris, France, 2010, pp. 2019-2022.
- [24] S. J. Martin, Gregory C. Frye, Antonio J. Ricco, and Stephen D. Senturia, "Effect of surface roughness on the response of thickness-shear mode resonators in liquids," *Analytical Chemistry*, vol. 65, pp. 2910-2922, 1993.
- [25] E. Ashley and J. Niebauer, *Cardiology Explained*. London: Remedica; 2004. Chapter 4, Understanding the echocardiogram. [Online]. Available: <https://www.ncbi.nlm.nih.gov/books/NBK2215/> [retrieved: August, 2021].
- [26] M. Rahman, J. Hernandez, and S. Chowdhury, "An improved analytical method to design CMUTs with square diaphragms," in *IEEE Transactions on Ultrasonics, Ferroelectrics, and Frequency Control*, vol. 60, no. 4, pp. 834-845, April 2013.
- [27] R. Manwar, "A BCB Diaphragm Based Adhesive Wafer Bonded CMUT Probe for Biomedical Application," Ph.D. dissertation, Dept. of Electrical and Computer Engineering, Univ. of Windsor, Windsor, ON, Canada, 2017.
- [28] F. Pavlo, "Capacitive micromachined ultrasonic transducer (cMUT) for biometric applications," Master's Thesis, Dept. of Nanoscience and Technology, Chalmers University of Technology, Göteborg, Sweden, 2012.
- [29] R. Manwar, L. Arjunan, M. Ahmadi, and S. Chowdhury, "Resonant frequency calculation of square diaphragms: A comparison," in *Proc of IEEE 6th Latin American Symposium on Circuits & Systems (LASCAS)*, Montevideo, Uruguay, 2015, pp. 1-4.